Numerical and Experimental Characterization of the Thermal Behavior of Complex Fenestrations Systems Under Dynamic Conditions

Ingrid Demanega – Eurac Research, Bozen-Bolzano, Italy – ingrid.demanega@eurac.edu
Giuseppe De Michele – Eurac Research, Bozen-Bolzano, Italy – giuseppe.demichele@eurac.edu
Martin Hauer – Bartenbach GmbH, Aldrans, Austria – martin.hauer@bartenbach.com
Stefano Avesani – Eurac Research, Bozen-Bolzano, Italy – stefano.avesani@eurac.edu
Giovanni Pernigotto – Free University of Bozen-Bolzano, Italy – giovanni.pernigotto@unibz.it
Andrea Gasparella – Free University of Bozen-Bolzano, Italy – andrea.gasparella@unibz.it

Abstract

Complex Fenestration Systems (CFS) with different types of shading devices are widely used to enhance the building envelope's energy efficiency and the occupants' visual and thermal comfort. These technologies are characterized, among other features, by advanced shading systems, with for example complex geometries and highly reflective surfaces, which introduce a performance dependence on the angle of incidence of solar radiation. This peculiarity has to be covered by adequate thermal and optical models. However, the current most widespread thermal models, based on the standard ISO 15099 and implemented in the main building energy simulation tools, have shown some restrictions in their applicability for CFS. In addition to this, professionals of the façade construction industry are interested in assessing the components' critical temperatures and the performance of the fenestration system under real dynamic operating conditions and in representative extreme conditions. In this framework, this study has investigated a new modelling approach for the thermal characterization of CFS under dynamic conditions by comparing simulation results with in-situ measurements of a triple-glazed window with integrated commercial blinds installed at the Free University of Bozen-Bolzano, Italy. The numerical assessment of the thermal behaviour of CFS was based on CFD simulations with the separately computed effect of solar radiation. The experimental characterization was performed with several instruments, such as conventional heat flux plates and a temperature-controlled in-situ measurement device to determine the undisturbed, transient heat flux through transparent components. From the comparison, a good correspondence between numerical and experimental results emerged and both approaches appraised the inertial effect of the fenestration system on the solar heat gain. Finally, it was observed that accurate optical modelling, together with CFD simulation, made it possible to compute the solar absorption and its significant impact on the fluid flow in the cavity, the components' temperatures and the solar gains.

1. Introduction

Transparent components and shading devices, designed in an optimal way, are crucial to increase the building envelope's energy efficiency and the exploitation of natural lighting. In recent years, complex shading systems, which aim to enhance occupants' visual and thermal comfort while reducing the building energy consumption, have been introduced. *The term 'Complex Fenestration System' (CFS) refers to all window technologies, including solar and light scattering or reflecting components. Their optical and thermal properties are described using a complex dependence on the angle of incidence and wavelength of the solar radiation* (Kuhn et al., 2011). Examples of these technologies are daylight redirecting systems, venetian blinds with complex geometries and highly reflective surfaces and prismatic layers. Indeed, the dependence on the angle of incidence allows for an improved management of solar radiation (Konis and Selkowitz, 2017). However, due to their complex nature, adequate models to evaluate Complex Fenestration systems' thermal and optical behaviour are required. For the optical characterization of CFS, the available models, based on the Bidirectional Scattering Distribution Function (BSDF), have already reached a high level of accuracy and are

widely used to perform daylight analysis. The procedure for calculating the thermal performance of glazing and shading systems is described in the international standard ISO 15099 (ISO, 2003). The standard approach, implemented in the main simulation tools, has restrictions in the applicability of complex system geometries or particular types of coatings, such as highly reflective ones (Demanega et al., 2018). Indeed, the ISO 15099 considers standard blind geometries, such as solar screens or venetian blinds with flat geometries and refers to diffusely reflecting surfaces. Addressing these standard technologies, the computation of the convective heat transfer through the window cavities is performed with a pressure drop model and applied to a layer-by-layer approach. This assumes the shading device is a layer parallel to the glass pane and has certain opening characteristics. However, this assumption is not adequate in the case of venetian blinds or other particular types of shading devices with large openings (Hart et al., 2017). Furthermore, the standard algorithms do not account for the heat capacity and thus the thermal inertia of the fenestration system despite it being an important aspect when characterizing the window system under dynamic conditions. In addition, professionals in the construction industry claim it is necessary to assess the components' critical temperatures and the heat flow through CFS under real operating conditions.
This study therefore aims to investigate a new modelling approach for the thermal characterization of CFS under dynamic conditions by comparing simulation results with in-situ measurements of a commercial system installed at the Free University of Bozen-Bolzano, Italy.

2. Simulation and Experiment

2.1 CFS Typology

The analyzed fenestration system was a commercial triple-glazed window composed of two sealed cavities and curved blinds with highly reflective surfaces integrated in the exterior cavity (Fig. 1). The thickness of the blinds was 0.2 mm, the width 15.9 mm and the pitch 12 mm. The analysis was done with a fixed slat inclination of 75° corresponding to a closed position. The exterior and central glasses were float glasses, while the interior glass was laminated. The geometric and thermal parameters of the window system are listed in Tables 1 and 2. On face 3 (the exterior side of the central glass pane) and face 5 (the exterior side of the interior glass pane) a low-emissivity coating was placed with an emissivity of 0.037. Both cavities were filled with a gas mixture of 90 % argon and 10 % air. This fenestration system was mounted on the west façade of the Living Labs inside the Free University of Bozen-Bolzano.

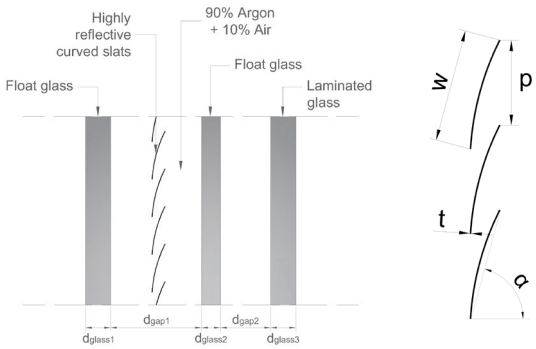

Fig. 1 – Layout of the Complex Fenestration System

Table 1 – CFS geometric parameters

Symbol	Parameter	Value
dglass1	Glass 1 width	8 mm
dgap1	Cavity 1 width	29 mm
dglass2	Glass 2 width	6 mm
dgap2	Cavity 2 width	16 mm
dglass3	Glass 3 width	8.76 mm
w	Blind width	16 mm
t	Blind thickness	0.2 mm
p	Pitch	12 mm
α	Blind tilting	75 °
H	Cavity height	0.9 m

Table 2 – CFS thermal parameters

Symbol	Unit	Cavity	Blind	Glass1/2	Glass3
λ	W/m/K	f(T)	100	1.0	0.757
c_p	J/kg/K	f(T)	900	820	820
ϱ	kg/m³	f(p,T)	2700	2500	2500
ε_f	-	-	0.150	0.037	0.037
ε_b	-	-	0.450	0.84	0.84

2.2 Modelling Approach

The thermal performance of the CFS is assessed by means of a new modelling approach, in which the fraction of absorbed solar radiation is calculated apart from the fluid flow and heat transfer and then included in a CFD simulation (Demanega et al., 2018). In this procedure solar radiation is treated with a detailed optical model based on ray tracing using the software Radiance (Ward, 1994); the resulting absorbed fraction of solar radiation is included in a comprehensive thermal modelling that couples heat transfer and fluid flow in a CFD simulation performed with the Finite Element (FE) software COMSOL Multiphysics. The simulation is done using time-dependent measured boundary conditions in terms of temperatures and solar irradiance. The computed heat flux is then compared with the in-situ measurements.

2.2.1 Solar radiation modeling

The optical modeling is required to compute the fraction of solar radiation absorbed by each solid element of the fenestration system. The highly reflective surface of the blinds and the curved geometry require a detailed modeling approach in order to appraise the angular dependent behavior. Thus, the analysis was carried out with the ray tracing software Radiance and a modified version of the Three-Phase Method (McNeil, 2014) that describes the way light passes through a fenestration system. Indeed, for this application, the scope was not the computation of the transmitted light but the absorbed radiation. The measured direct and diffuse horizontal irradiances were therefore used to generate the sky matrix to be coupled with the Bidirectional Scattering Distribution Function (BSDF) of the analyzed fenestration system via the daylight matrix, which takes into consideration the real building and surrounding geometry in order to calculate the absorbed share of solar radiation for each time-step.

2.2.2 CFD and thermal modelling

The computation of the coupled heat transfer and fluid flow was done with a CFD simulation using the software COMSOL Multiphysics. Some assumptions for this application were made. In particular, the real geometry was reduced to a vertical section (2D domain). This simplification is justified by the studies performed by Pasut and De Carli (2012) with the conclusion that modeling the entire 3D geometry of the fenestration system, instead of a 2D one, does not provide a substantial improvement in the results, considering the required additional effort. The fluid was considered as incompressible and the buoyancy driven flow was solved with the Boussinesq approximation (Versteeg and Malalasekera, 2005). Due to the low Grashof number (Gr ≈ 10e4), which measures the ratio of the buoyancy to viscous forces (Equation 1), the fluid flow was considered laminar (Schlegel, 2015).

$$G_r = \frac{g\,\beta\,\rho^2 \Delta T\, L^3}{\mu^2} \qquad (1)$$

The long-wave radiation exchange between the solid elements of the CFS was computed with the radiosity method, the so-called surface-to-surface method (van Eck et al., 2016), which depended on the temperature of the single parts, the view factors and the emissivity of the surfaces. For the CFD simulation an adequate mesh was created: a structured quad mesh was used for the solid domains, while a free triangular grid was applied to the fluid domain. Furthermore, the mesh was refined near the boundaries to guarantee a smooth transition from the non-zero fluid velocity to the zero velocity on the surface. To evaluate the mesh quality and guarantee that the solution is independent from the grid size, a mesh sensitivity analysis was carried out: considering the U-value (thermal transmittance) as control parameter, the mesh was refined until no further significant improvement in the U-value result was reached. The final mesh is shown in Fig.s 2 and 3. The total number of elements amounts to 56 281.

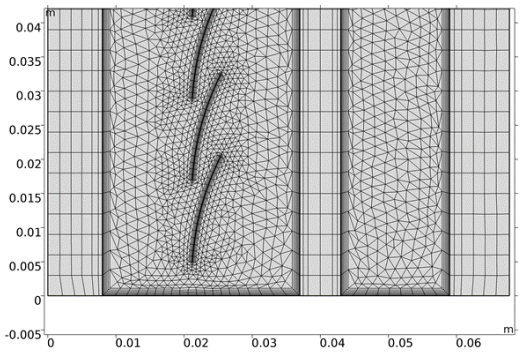

Fig. 2 – Final mesh of the Complex Fenestration System

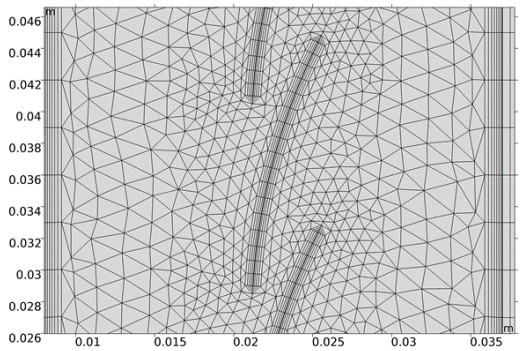

Fig. 3 – Final mesh around the blinds of the CFS

For the CFD simulation the boundary conditions in terms of measured internal and external surface temperatures were assigned, in addition to the pre-calculated solar absorption that was set up as heat source. The boundary conditions were measured during a sunny clear sky day in February 2018 from 9 am to 6 pm and assigned to the CFD model with a time-step of 300 s.

The conjugate heat transfer and fluid flow simulation was run with a time-dependent study and using a fully coupled solver. The simulation of each time-step was considered converged if the relative residuals of the continuity, momentum and energy equations were less than 10e-3.

From the CFD simulation a temperature, pressure and velocity distribution over the fenestration system and for all the time-steps resulted. This made it possible to compute the total heat fluxes on all the grid points of the room-side face of the CFS. An integration of the heat flux over the total height of the interior glazing, except for the top and bottom extremes which had an extension of 10 % of the total height, was done. This made it possible to reproduce a similar condition as the measurement in which the heat flux was measured mainly at the center of the glazing, thus it did not account for the border effects.

2.3 In-Situ Measurements

In-situ measurements of the CFS installed on the west façade of the Living Labs of the Free University of Bozen-Bolzano were performed during a period of two weeks in February 2018. After analysing the experimental data, a sunny clear sky day was selected for the comparison with the CFD simulation. Different parameters were measured in order to characterize the thermal behaviour of the window system: internal and external air temperature near the façade, internal and external glazing surface temperature in different positions, total heat flux on the internal side, global and diffuse horizontal irradiance outside and total vertical irradiance on the façade.

For all the temperature measurements T-type thermocouples were used and their output voltage was read by a Datataker DT80 datalogger equipped with an internal reference. Those mounted on the exterior glazing surface were shielded from direct solar radiation using a silver tape to prevent the thermocouple from being heated up by direct irradiance. On the internal side, it was not necessary to shield the thermocouples since the closed position of the blinds prevented direct solar radiation hitting them. The total heat flux on the internal glazing surface was measured in two ways: conventional heat flux plates Hukseflux HFP01 and a temperature-controlled measurement device to determine the undisturbed, transient heat flux through transparent components (Hauer, 2017). This novel in-situ heat flux device (Fig. 4) measures the heat flow by means of a heat flux plate that is fixed slightly detached on the inner glazing surface via cupping vessels. In contrast to standard heat flux plates, this apparatus is continuously cooled through temperature-controlled Peltier elements, which prevent overheating of the device resulting from solar absorption, and therefore misleading measurement results.

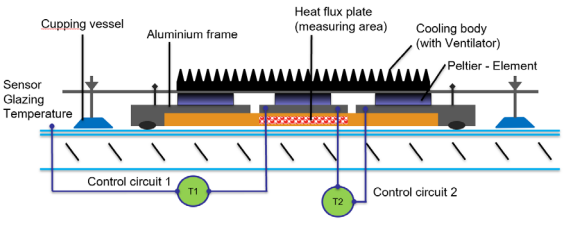

Fig. 4 – Section view of the in-situ heat flux device (Hauer, 2017)

The global and diffuse horizontal irradiance was measured with two Kipp&Zonen CMP11 thermopile pyranometers. With the use of the sole pyranometer placed on a horizontal surface, the global horizontal irradiance was measured, while to record the amount of diffuse irradiance a pyranometer with a solar tracker was used. In addition to the horizonal pyranometers, a Delta-T Devices SPN1 Sunshine Pyranometer was installed vertically on the external side of the west façade to evaluate the time-shift between the incident solar radiation and the measured heat flux on the internal side.

Fig. 5 shows all the measurement instruments installed on the analyzed fenestration system and Table 3 reports the instrument specifications.

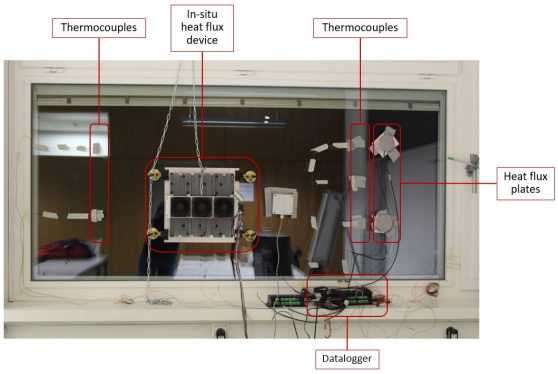

Fig. 5 – Measurement setup for the CFS

Table 3 – Instrument specifications

Parameter	Instrument	Accuracy
Temperature	T-type Thermocouple	± 0.3 °C (k = 2)
Heat flux	Hukseflux HFP01 Heat flux plate	± 3 % (k = 2)
Heat flux	In-situ heat flux device	< ± 10 %
Horizontal irradiance	Kipp&Zonen CMP11 Pyranometer	± 2 % Daily total
Vertical irradiance	Delta-T Devices SPN1 Sunshine Pyranometer	±8% ±10 W/m² Individ. readings

3. Results and Discussion

The measurements on the fenestration systems provided several data and the inside and outside surface and air temperatures for a sunny clear sky day were compared. Fig. 6 shows the trend of the external air temperature near the façade and the external surface temperatures measured at two different heights. During the day, the surface temperature is affected by a significant variation, starting from 1.0 °C in the morning and reaching 36.8 °C in the afternoon. In contrast, on the internal side the variation over the day is not so large due to the thermal insulation and inertia of the fenestration system and the controlled internal air temperature (Fig. 7).

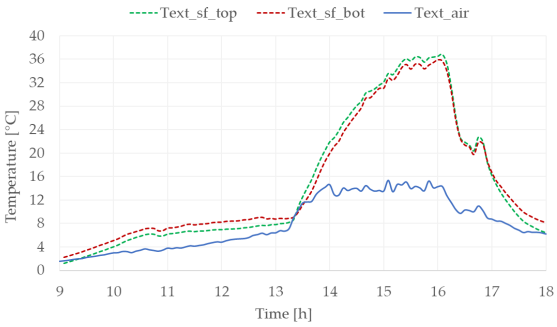

Fig. 6 – External air and surface temperatures for the CFS

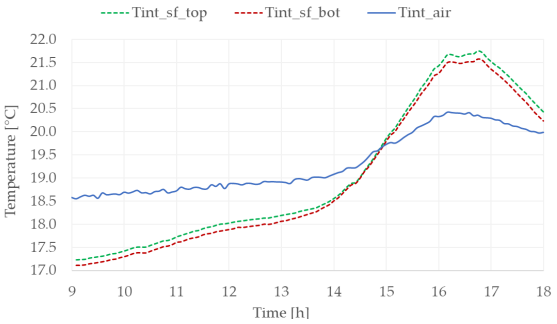

Fig. 7 – Internal air and surface temperatures for the CFS

A comparison between the total heat flux on the room-side face measured with the two types of instruments and the simulated heat flux was performed in order to characterize the thermal behaviour of the CFS under dynamic conditions and to validate the simulation against the measurement approaches (Fig.s 8 and 9). From this comparison, a good correspondence between simulated and measured heat flux emerged. In particular, during the period in which the system is heated up by direct solar radiation the correspondence was very good although the simulated values showed some steep fluctuations, which could be due to numerical errors. However, in the morning, when the façade is not affected by direct solar radiation, the simulated

heat flux had the same trend as the measured heat flux but it was underestimated. It can be noted that this difference decreased over the course of the morning, hence it could be a result of the fact that the simulation was initialized with the boundary conditions measured at the first instance of the comparison (i.e. 9 am) and did not consider the period before.

The peak heat flux resulting from the simulation amounted to 13.7 W/m², while the heat flux plates measured a peak value of 12.9 W/m² and the in-situ heat flux device of 11.0 W/m². The largest divergence between measurement results was recorded after sunset: in this time frame, an offset of up to 4 W/m² between the values measured by the two devices occurred. This deviation could be caused by a combination of a number of effects, such as the different response time to temperature variations of the two instruments. Indeed, the in-situ heat flux device showed a very fast reaction due to the Peltier coolers. In this period, the calculated heat flux was closer to the one measured by the heat flux plates. Beyond this, it is interesting to note that both the numerical model and in-situ measurements perceived the inertial effect of the glazing unit, which caused a time-shift of around one hour between the instance of the peak irradiance and that of maximum solar gain.

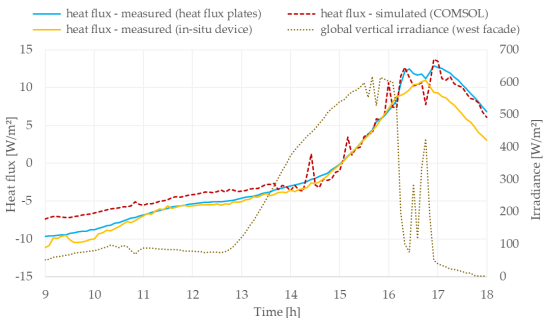

Fig. 8 – Comparison of simulated and measured heat flux through the CFS

Fig. 10 shows the relative deviations between the numerical and experimental results: in the case of positive – entering – heat flux, the relative deviations for the heat flux plates were mostly within 10 %, while they were around 20 %, in some instances even higher, in the case of the in-situ heat flux device due to the deviation of the results after sun-set. In this period, the in-situ device underestimated the solar gains compared to the heat flux plates and the simulation results. Analysing the negative – exiting – heat flux, the relative deviation was mainly within 20 % for low heat fluxes and around 20 % for higher values.

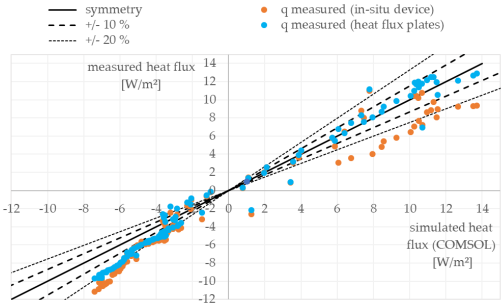

Fig. 9 – Deviations between simulated and measured heat flux

The discrepancy between simulated and measured data can be described through the RMSE (Root Mean Square Error) and MAE (Mean Absolute Error) defined as:

$$RMSE = \sqrt{\frac{\sum_{i=1}^{n}(q_{meas,i}-q_{sim,i})^2}{n}} \quad (2)$$

$$MAE = \frac{\sum_{i=1}^{n}|q_{meas,i}-q_{sim,i}|}{n} \quad (3)$$

The resulting mean errors RMSE and MAE for the in-situ heat flux device and the heat flux plates are reported in Table 4.

Table 4 – Comparison of simulation and measurement results

	RMSE [W/m²]	**MAE [W/m²]**
Simulation vs measurements (in-situ device)	2.16	1.81
Simulation vs measurements (heat flux plates)	1.45	1.24

From the RMSE and the MAE a good correspondence between numerical and experimental results emerged. However, these indicators confirmed a better correspondence of the simulation results with the heat flux plate measurements than the in-situ heat flux device for this configuration of glazing system and blind inclination. It should be noted that

the closed position of the blinds prevented direct solar radiation from reaching the measurement devices and overheating them. When there were different – more open – blind positions, the heat flux plates can become overheated and disturbed by the absorption of direct solar radiation. This was avoided with the in-situ heat flux device, mounted slightly detached from the glazing and cooled by temperature-controlled Peltier elements.

In addition to the heat flux, the comprehensive modelling of heat transfer and fluid flow coupled with the effect of solar radiation makes it possible to account for the components' temperatures that can be reached inside the sealed cavity. The absorption of solar radiation on the blinds and the glass panes significantly increases their temperature. The closed cavity does not enhance the heat dissipation, thereby inducing the filling gas temperature to rise. For this glazing configuration, the blinds in the upper part of the cavity can reach temperatures of around 50 °C, even in winter conditions with a maximum external air temperature of 15 °C.

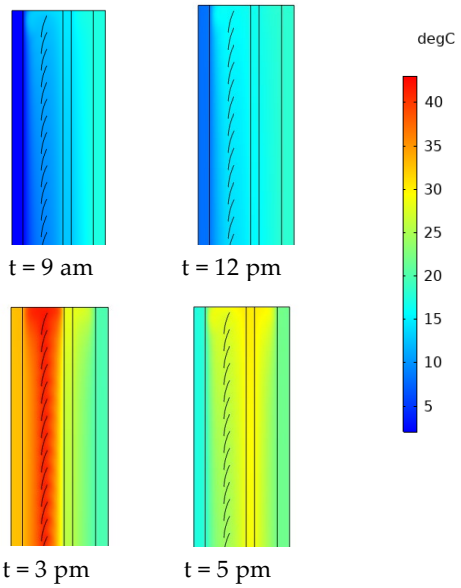

Fig. 10 – Temperature distribution within the CFS at different times

4. Conclusion

The results discussed show that the coupling of CFD simulations with the separately computed effect of solar radiation is a valid modelling approach for assessing the thermal performance of Complex Fenestration Systems under dynamic conditions. This modelling approach could be appropriate for a detailed analysis of fenestration systems in order to assess specific properties, for instance secondary heat fluxes, maximum temperatures of certain components of the glazing unit or fluid flow rates in the cavity. From the numerical modelling of CFS, it emerged that the solar absorption has a significant impact on the fluid flow in the cavity, the solar heat gains and the temperatures of the components. Thus, in addition to a CFD-based approach that considers the effect of the fluid flow, an accurate optical modelling is essential to appreciate the glazing and shading complexity. Furthermore, the numerical and experimental characterization of the thermal behaviour of CFS under dynamic conditions provided evidence of the inertial effect of fenestration systems causing a time-shift of around one hour between the instance of the peak irradiance and that of maximum solar gain of the room.

For this glazing configuration with blinds in a closed position, numerical results in terms of heat fluxes are confirmed by experimental measurements, using both conventional heat flux plates and a temperature controlled in-situ heat flux measurement device.

Further analysis will be done in order to validate the modelling approach for different blind positions and apply it to naturally ventilated cavities. In this case, the fluid flow within the cavities is expected to have an even greater impact on the overall heat transfer and thus the performance of the fenestration system.

Acknowledgement

This study has been developed in the framework of the research activities of the project FACEcamp n. ITAT1039, funded by European Regional Development Fund and Interreg ITA AUT programme and by the project Klimahouse and Energy Production in the framework of the programmatic-financial agreement with the Autonomous Province of Bozen-Bolzano of Research Capacity Building of the Free University of Bozen-Bolzano.

Nomenclature

Symbols

G_r	Grashof number (-)
g	Gravitational acceleration (m/s²)
β	Volume expansivity (1/K), β=1/T for ideal gases
ρ	Density (kg/m³)
ΔT	Temperature difference (K)
L	Characteristic length (m)
μ	Dynamic viscosity (Ns/m²)
$q_{meas,i}$	Measured heat flux at timestep i (W/m²)
$q_{sim,i}$	Simulated heat flux at timestep i (W/m²)

References

Demanega, I., G. De Michele, G. Pernigotto, S. Avesani, F. Babich, A. Gasparella. 2018. "CFD and ray tracing to evaluate the thermal performance of Complex Fenestration Systems." *Proceedings of the 2018 Building Simulation and Optimization Conference in Cambridge*, 460-466.

Hart, R., H. Goudey, D. C. Curcija. 2017. "Experimental validation and model development for thermal transmittances of porous window screens and horizontal louvred blind systems." *Journal of Building Performance Simulation* 11(2), 1–15.

Hauer, M. 2017. "Model Development and Validation for an Integrative Thermal and Daylight Evaluation of Complex Fenestration Systems in Building Performance Simulations". PhD Dissertation, Universität Innsbruck. Institut für Konstruktion und Materialwissenschaften, AB Energieeffizientes Bauen.

ISO. 2003. *ISO 15099:2003: "Thermal performance of windows, doors and shading devices — Detailed calculations"*.

Konis, K., S. Selkowitz. 2017. *Effective daylighting with high-performance facades: emerging design practices*. Springer.

Kuhn, T. E., S. Herkel, F. Frontini, P. Strachan, G. Kokogiannakis. 2011. "Solar control: A general method for modelling of solar gains through complex facades in building simulation programs." *Energy and Buildings* 43, 19–27.

McNeil, A. 2014. "The Three-Phase Method for Simulating Complex Fenestration with Radiance". LBNL. https://www.radiance-online.org/learning/tutorials/Tutorial-ThreePhaseMethod.pdf

Pasut, W., M. De Carli. 2012. "Evaluation of various CFD modelling strategies in predicting airflow and temperature in a naturally ventilated double skin façade." *Applied Thermal Engineering* 37, 267–274.

Schlegel, F. 2015. "Using the Boussinesq Approximation for Natural Convection." COMSOL Blog. Accessed 2019 Sep 19. https://www.comsol.com/blogs/using-the-boussinesq-approximation-for-natural-convection/

Van Eck, R. 2016. "Surface to Surface Radiation Benchmarks." *Proceedings of the 2016 COMSOL Conference* in Munich, 1-6.

Versteeg, H. K., W. Malalasekera. 2005. *An introduction to computational fluid dynamics: the finite volume method*. Harlow: Pearson/ Prentice Hall.

Ward, G. 1994. "The RADIANCE Lighting Simulation and Rendering System." *Proceedings of the 21st annual conference on Computer graphics and interactive techniques*, 459-472.